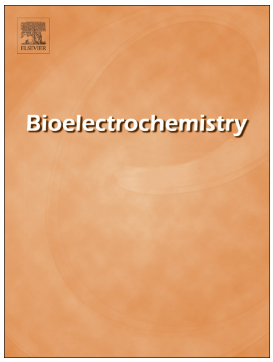

Effect of external resistance on the sensitivity of microbial fuel cell biosensor for detection of different types of pollutants

Yue Yi, Beizhen Xie, Ting Zhao, Zhaoming Li, Devard Stom, Hong Liu

PII: S1567-5394(18)30218-4
DOI: doi:10.1016/j.bioelechem.2018.09.003
Reference: BIOJEC 7205

To appear in: *Bioelectrochemistry*

Received date: 18 May 2018
Revised date: 5 September 2018
Accepted date: 6 September 2018

Please cite this article as: Yue Yi, Beizhen Xie, Ting Zhao, Zhaoming Li, Devard Stom, Hong Liu , Effect of external resistance on the sensitivity of microbial fuel cell biosensor for detection of different types of pollutants. Biojec (2018), doi:10.1016/j.bioelechem.2018.09.003

Effect of External Resistance on the Sensitivity of Microbial Fuel Cell Biosensor for Detection of Different Types of Pollutants

Yue Yi[a,b], Beizhen Xie[a,b,*] xiebeizhen@buaa.edu.cn, Ting Zhao[a,b], Zhaoming Li[a,b], Devard Stom[c], Hong Liu[a,b]

[a]Institute of Environmental Biology and Life Support Technology, School of Biological Science and Medical Engineering, Beihang University, Beijing 100191, China

[b]International Joint Research Center of Aerospace Biotechnology&Medical Engineering, Beihang University, Beijing 100191, China

[c]Institute of Biology, Irkutsk State University, Irkutsk 664025, Russia

[*]Corresponding author.

Abstract

The relatively poor sensitivity is the main bottleneck restricting the application of microbial fuel cell biosensor (MFC-biosensor) for toxicity monitoring. Previous studies have shown that external resistance (R_{ext}) had an obvious effect on sensor sensitivity. However, these studies reported different results and the reason of this discrepancy was not clear. The objective of this research was to observe the effect of R_{ext} on sensor sensitivity when detecting different types of pollutants and reveal its microbiological mechanism. Results demonstrated that the optimal R_{ext} of MFC-biosensor varied with the type of pollutants. The optimal values for detecting avermectins, tetracyclines and heavy metals were 100 Ω, 330 Ω and 680 Ω, respectively. This discrepancy was mainly due to the visible differences in anodic microbial communities at different R_{ext} settings. Both *Azospirillum* and *Acinetobacter* were susceptible to Cd and Pb, occuping 19.20% of the anodic microbial population in 680 Ω MFC-biosensor. *Pseudomonas* accounted for 10.73% in 330 Ω MFC-biosensor and possessed the sensitivity to tetracyclines. As for 100 Ω MFC-biosensor, the avermectin-intolerant *Ocillibacter* made up 2.55% of the anodic microbial community. This study indicated that the R_{ext} of MFC-biosensor should be optimized according to the potential pollutants.

Graphical Abstract

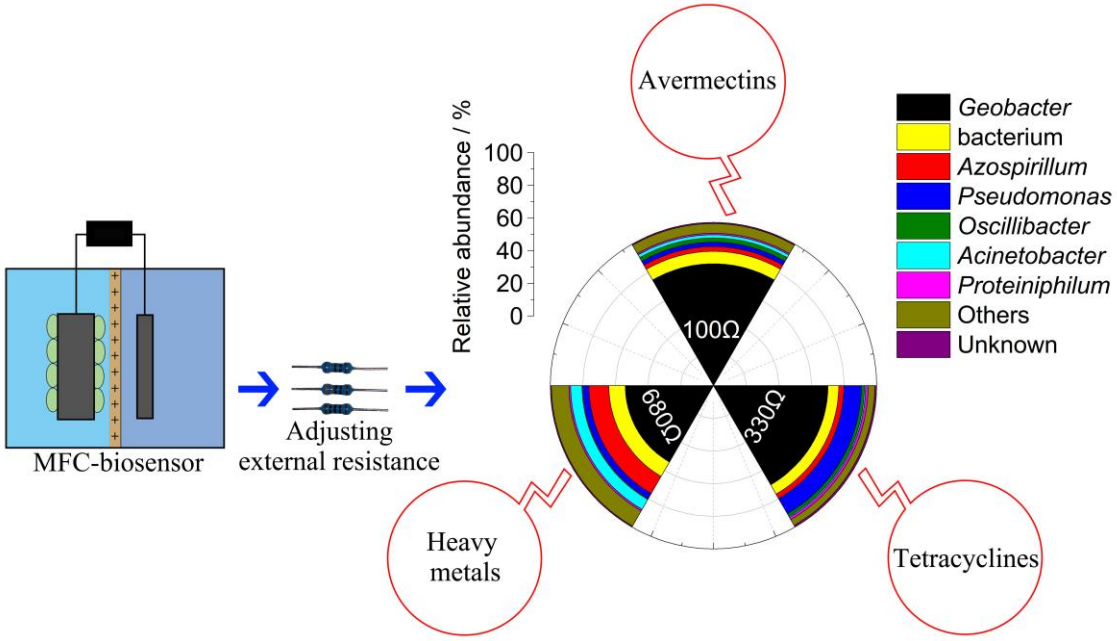

Keywords

microbial fuel cell, biosensor, heavy metal, antibiotic, external resistance, microbial community

1. Introduction

Water supply safety is critical for urban construction and social stability. With the continuous development of global industrialization, the type and quantity of toxic pollutants in aquatic environment are increasing annually. Reliable methods of water quality monitoring are indispensable for the guarantee of water supply safety. Physicochemical methods, which are broadly applied in conventional monitoring of water quality, are highly sensitive and accurate. However, these methods are inadequate to detect unconventional pollutants and fail to provide a timely warning of water pollution. Moreover, these methods cannot give an indication of biological toxicity. Generic biosensors can compensate for the deficiencies of physicochemical methods. Fish, algae, invertebrates and bacteria are suggested as common indicator organisms [1]. Among various types of biosensors, microbial fuel cell biosensors (MFC-biosensors) have attracted growing interest in the area of water quality alert in the last decade. Compared with other biosensors, MFC-biosensor can be self-sustainable without the requirements of additional signal transducer devices and special chemicals, which makes it a promising application in water quality monitoring [2, 3].

MFC is a device which utilizes electricigens as catalysts and simultaneously converts chemical energy from organic matter into electricity [4]. Presence of toxic agents can inhibit the activity of electricigens, and further leads to a decay in output signal. Hence water quality can be monitored in real-time by measuring the change of MFC output voltage. The first biomonitoring system using MFC was reported by Kim et al [5]. They installed the system at the inlet of a wastewater treatment plant and found that toxic substances including Pb^{2+} and Cd^{2+} could inhibit MFC current, demonstrating the feasibility of monitoring biotoxicity by MFC. Since then, a series of constructional and operational parameters including external resistance (R_{ext}) [6], configuration [7], electrode material [8], contact time [9], shear rate [10] and flow mode [11] were optimized to enhance sensor sensitivity.

Among these parameters, R_{ext} is considered to be an important factor which directly impacts the power generation of MFC-biosensor and further affects sensor sensitivity [12, 13]. An early study reported that increasing R_{ext} settings (100 Ω, 470 Ω, 1000 Ω) had an adverse effect on the sensitivity of MFC-biosensor for detecting sodium dodecyl sulfate [6]. When monitoring a heavy metal shock induced by Cu^{2+}, Jiang et al. [11] observed that the sensitivity increased firstly, and then reduced with the decrease of R_{ext} from 3000 Ω to 50 Ω. Another study conducted by Yi et al. [14] revealed that MFC-biosensor designed for testing Cd^{2+} obtained the highest sensitivity when R_{ext} was equal to 500 Ω, and higher or lower R_{ext} settings would both deteriorate the sensitivity. Interestingly, these studies reported inconsistent effects of R_{ext} on sensor sensitivity when monitoring different types of pollutants. This phenomenon suggested that the optimal R_{ext} might vary with the type of pollutants but a comparison about the optimal R_{ext} for organic and inorganic pollutants has not been revealed yet. Besides, the influencing mechanism of R_{ext} was not clear. It was found in all the previous studies that R_{ext} had similar effects on MFC power generation. This could not explain the different effects of R_{ext} on sensor sensitivity when detecting various pollutants. Therefore, the

mechanism needed to be further studied.

From the microbiological perspective, R_{ext} had a significant effect on anodic community structure [15, 16]. The species and distribution of electricigens had obvious differences under different R_{ext} values [17, 18]. Considering the discrepancies in microbial resistance to different types of toxic pollutants, it could be deduced that the optimal R_{ext} might vary with the type of pollutants. That is to say, R_{ext} could impact the microbial community structure of MFC-biosensor and further affects its sensitivity.

In this research, our objective was to investigate the effect of R_{ext} on sensor sensitivity when detecting different types of pollutants and reveal its microbiological mechanism. For this purpose, MFC-biosensors loaded with different R_{ext} values were constructed. After steady-operation, toxic pollutant tests were performed to study the relationship between optimal R_{ext} and pollutant type. Three types of pollutants, including heavy metals, tetracyclines and avermectins, were tested and each type was represented by two pollutants. Then, two types of combined contaminations represented by the binary metal mixture and metal-tetracycline composite pollutant were examined to assess the change of optimal R_{ext} induced by combined contamination. Finally, high-throughput sequencing technology was employed to investigate the anodic microbial communities established under optimal R_{ext} values for different pollutants and the changes of community structures to toxic shocks.

2. Materials and Methods

2.1 Chemicals and reagents

Analytical reagents $3CdSO_4 \cdot 8H_2O$ and $PbCl_2$ were purchased from Beijing Lanyi Chemical Products Co., Ltd., China. Chlortetracycline hydrochloride (CTC) and oxytetracycline hydrochloride (OTC) were acquired from Dalian Ronghai Biological Technology Co., Ltd., China. Avermectin (AVM) and ivermectin (IVM) were obtained from Wuhan Bioland Biological Technology Co., Ltd., China. $3CdSO_4 \cdot 8H_2O$, $PbCl_2$, CTC, OTC were individually dissolved in deionized water to prepare stock solutions while AVM and IVM were dissolved in absolute methanol respectively. The concentration of the stock solution for each toxic pollutant was 1.0 g/L and all were preserved in 4 ^{o}C refrigerator for further use. Anolyte and catholyte were prepared prior to use. The fresh anolyte used in this study consisted of 5.85 g NaCl, 0.13 g KCl, 0.31 g NH_4Cl, 6.08 g $NaH_2PO_4 \cdot 2H_2O$, 21.83 g $Na_2HPO_4 \cdot 12H_2O$, 12.50 mL trace minerals solution and 5.00 mL vitamin solution in 1.00 L deionized water [19]. The catholyte consisted of 5.85 g NaCl, 6.08 g $NaH_2PO_4 \cdot 2H_2O$ and 21.83 g $Na_2HPO_4 \cdot 12H_2O$ in 1.00 L deionized water. During the start-up process, sodium acetate (NaAc) was added to fresh anolyte as carbon source to achieve a final concentration of 0.82 g/L. When toxic pollutants tests were performed, the concentrations of NaAc in non-toxic and toxic anolyte were switched to 0.082 g/L to enhance sensor sensitivity [20]. Toxic and non-toxic anolyte was prepared by adding a certain volume of toxic stock solution and the same volume of solvent in fresh anolyte, respectively.

2.2 MFC construction and start up

Fifteen MFCs (MFC1-15) of optimized configuration (Figure A.1) were constructed and divided into two groups. MFC1-9 with different external loads (100 Ω,

330 Ω, 680 Ω), were constructed to optimize R_{ext} for various pollutants. For each R_{ext} value, three MFCs were set to test the reproducibility of results and perform statistics analysis. The other group (MFC10-15) was used for subsequent analysis of anodic microbial community. All parameters except for R_{ext} were consistent in each MFC. The working volume of the anodic chamber was 13 mL while the cathodic chamber was 25 mL. Proton exchange membrane (Nafion 117, Hesen Electric Corporation, China) was used to divide the two chambers. A 3.0 cm×2.5 cm piece of carbon cloth (HCP330, Hesen Electric Corporation, China) treated by ammonia [21] was used as anode. Cathode consisted of two 2.0 cm×2.0 cm pieces of carbon paper containing 0.5 mg/cm^2 Pt catalyst. Air was sparged into the catholyte to allow oxygen reduction on the cathode. To investigate the effect of R_{ext} on start-up process, the incubation conditions kept identical and the anolyte of each MFC was refreshed simultaneously. All the MFCs were inoculated with the effluent taken from an acetate-fed MFC using the same inoculum size of 30% (v/v). Each feed replenishment was performed by pumping anoxic fresh anolyte containing 0.82 g/L NaAc with a volume of 28.00 mL into anodic chamber. During the start-up process, the anolyte was forced to flow through the anodic electrode [11] with the application of self-circulation at a flow rate of 2 mL/min. All the MFCs were maintained at a temperature of 25.0±0.5 ^{o}C during all experiments.

2.3 Toxic pollutants tests

After the start-up process, the MFC-biosensors (MFC1-9) were fed with a continuous flow of influent and challenged with a series of toxic pollutants. The flow rate was maintained at 2 mL/min. The concentrations of organic pollutants (tetracyclines and avermectins) were 1.0 mg/L with reference to a previous study [5]. The concentration of Cd^{2+} as well as Pb^{2+} was 1.5 mg/L according to a previous study which indicated that electricigens were tolerant to heavy metals to a certain extent [22]. Combined contaminations consisted of two binary mixtures: 1.5 mg/L Pb^{2+} was mixed with 1.5 mg/L Cd^{2+} and 1.0 mg/L OTC respectively. The detection procedure comprised of three steps. Firstly, non-toxic anolyte was continuously pumped into the anodic chamber. Secondly, when the output voltage of each MFC-biosensor stabilized for more than two hours, the influent was switched to the toxic anolyte containing a certain concentration of target toxic pollutant and the exposure time was one hour. Finally, toxic anolyte was discharged from the anodic chamber and simultaneously non-toxic anolyte was continuously pumped to remove residual toxic pollutants inside the biofilm. Each toxic shock was performed in triplicate for one R_{ext} setting.

2.4 Microbial community analysis

To investigate the biological mechanism of the discrepancy in optimal R_{ext} values for various pollutants, six MFCs (MFC10-15) were constructed at the optimal R_{ext} settings of the six pollutants above, respectively. After the start-up process, non-toxic anolyte containing 0.082 g/L NaAc was continuously pumped into the anodic chamber for 15 days. Then sterilized scalpel was used to collect a 3.0 cm×0.3 cm piece of carbon cloth sample from the same position in the anode of each MFC. All the samples were stored at -80 ^{o}C refrigerator after quick-frozen with liquid nitrogen. Then each MFC was challenged with the toxic anolyte containing a certain concentration of target toxic

pollutant in the next seven days. The concentrations used here were identical to the above description. After exposure to toxic pollutants for seven days, anodic biofilms were all sampled again. Sampling technique and storage method were mentioned above.

DNA extraction of all the samples and the quality control of DNA samples were performed according to Xie et al. [23]. The hypervariable region V3-V4 of the 16S rRNA gene of all the samples was amplified by polymerase chain reaction using primers 338F (5'- ACTCCTACGGGAGGCAGCA-3') and 806R (5'-GGACTACHVGGGTWTCTAAT-3'). Each sample was sequenced by Illumina Hiseq platform at Biomarker Technologies Co., Ltd., China. Raw sequence data were filtered firstly and then high-quality sequences were clustered into operational taxonomic units (OTUs) at a similarity threshold value of 97% by QIIME software. At the classification level of OTU, Principal Coordinates Analysis (PCoA) was performed using the binary-jaccard algorithm by R software (3.5.1, The R Foundation for Statistical Computing, www.r-project.org) to analyze the differences among microbial communities formed under different R_{ext} settings.

2.5 Analysis

The output voltage of MFC was recorded at a sampling interval of 1s using a data acquisition system (USB-1608FS, Measurement Computing Corporation, USA). The internal resistance of MFC was characterized by electrochemical impedance spectroscopy (EIS). Before EIS measurement, the MFC was disconnected with the external resistor for at least 3h to obtain a stable open circuit voltage [24]. EIS was measured in the dual-electrode mode using electrochemical workstation (Zennium E, Zahner Company, Germany) at open circuit in a frequency range of 100 mHz to 10 KHz with a signal of 10 mV amplitude. EIS data was fitted with an equivalent circuit model (R_s+ CPE_1/R_1+CPE_2/R_2) according to a previous study [25]. R_s represented the ohmic resistance. R_1 and R_2 referred to the polarization resistance of cathode (R_c) and anode (R_a) respectively. Two constant phase elements (CPE_1 and CPE_2) were used to simulate nonideal capacitors. The inhibition ratio (IR) of output voltage was used to assess the sensitivity of MFC-biosensor in order to eliminate the interference of baseline signal in different MFCs [9, 26]. It was defined as the relative change of output voltage after toxic shock and calculated according to equation (1):

$$\mathrm{IR} = {}^{(V_n - V_t)}/_{V_n} * 100\% \quad (1)$$

where V_n was the voltage before the toxic shock and V_t was the voltage after exposure to the toxic pollutant for one hour. Optimal R_{ext} was determined when the maximum IR was picked out in the MFC-biosensors with different R_{ext} settings. Statistical analysis was conducted via SPSS Statistics 22. Significance test was used to analyze the responses of MFC-biosensors operated at different R_{ext} settings to each toxic pollutant via one-way analysis of variance and LSD multiple comparisons. The significant level was fixed at $p<0.05$.

3. Results and Discussion

3.1 Effect of external resistance on the start-up process and internal resistance

The evolution of MFC output voltage during the start-up process was presented in Fig. 1a. A recognizable voltage was observed immediately after the inoculation and it disappeared quickly in a short period of time. Then after a lag period of approximately 2000 minutes, the output voltages started to gradually increase, indicating the acclimatization process of electricigens to anodic environment. The long lag period was also reported by Zhang et al. [27]. This phenomenon might be due to that electricigens did not hold a dominant position in anodic microbial population during the lag period, which resulted in an incomplete extracellular electron transport process. Figure 1b showed the maximum voltage changes for each MFC in the first eight batches. When the deviation of maximum voltages between two batches was within ±5%, the completion of start-up process was confirmed. As shown in Figure 1b, the MFC loaded with 680 Ω completed the start-up process in the fourth batch while the MFC loaded with 100 Ω accomplished in the seventh batch. It was noted that the time needed for MFC to complete start-up process reduced with the increase of R_{ext}. A similar impact of R_{ext} on the start-up process was also observed by Lyon et al. [18]. This effect could be due to that R_{ext} affected anodic potential [27] and further modulated the growth of electricigens.

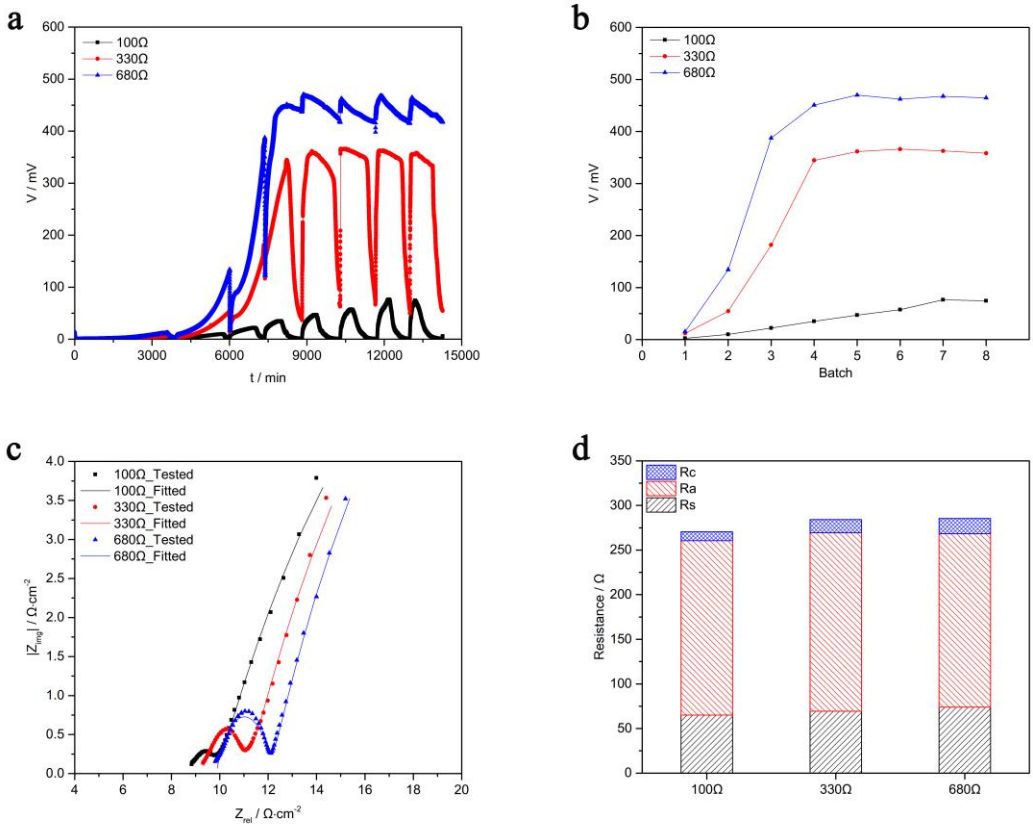

Figure 1. Effect of R_{ext} on the start-up process and internal resistance: (a) output voltages during the start-up process; (b) maximum output voltages in the first eight batches; (c) Nyquist plots of impedance spectra fitted to the equivalent circuit; (d) compositions of internal resistance obtained by model simulation.

EIS was tested after the start-up process of each MFC to evaluate the effect of R_{ext} on internal resistance. The fitting results were shown in Figure 1c and the compositions of internal resistance were presented in Figure 1d. It could be seen that the overall internal resistance showed minor differences under different R_{ext} values. Besides, R_a could reflect the electroactivity of anodic biofilm. According to the EIS test, the R_a of the MFCs loaded with 100 Ω, 330 Ω and 680 Ω were 195.4 Ω, 200.1 Ω and 194.5 Ω, suggesting the biofilm activities were similar under various R_{ext} values.

3.2 Effect of external resistance on sensor sensitivity

After the start-up process and steady operation for 15 days, MFC-biosensors (MFC1-9) were challenged with six pollutants and two combined contaminations to investigate the impact of R_{ext} on sensor sensitivity. When operated with non-toxic anolyte, all the MFC-biosensors generated stable voltages with fluctuation less than 5% (Figure A.2). Once exposed to CTC contaminated anolyte (in the 10th minute), the output voltages showed sharp decreases (Figure 2a). Similar results were also observed in the other pollutants tests, suggesting acute biological toxicity of the pollutants at examined concentrations to MFC-biosensors.

As shown in Figure 2b, the responses of the MFC-biosensors operated at various R_{ext} settings (100 Ω, 330 Ω, 680 Ω) showed significant differences when detecting tetracyclines. The IR to the shock of 1.00 mg/L CTC achieved 39.1±3.6% at 330 Ω, followed by 23.1±2.6% at 100 Ω and 15.4±1.8% at 680 Ω. Similar trend was also observed in the detection of OTC. However, the effect of R_{ext} on sensor sensitivity was different when examining other types of pollutants. Decreasing R_{ext} deteriorated the sensitivity to detect heavy metals but enhanced the sensitivity to avermectins (Figure 2c-d). Maximum IR values of 22.8±1.7% and 21.8±2.2% were observed at 680 Ω for 1.50 mg/L Cd^{2+} and Pb^{2+} shocks respectively while 17.8±1.9% and 18.0±2.1% for AVM and IVM at 100 Ω. Therefore, identical optimal R_{ext} was given for the same type of pollutants while distinct optimal R_{ext} for various types of pollutants. Parameters such as configuration design, shear rate and substrate concentration could affect the sensor sensitivity [7, 10, 20]. In this study, the configuration design, flow mode and test condition were identical except for the R_{ext} of MFC-biosensor. Meanwhile, the interference of baseline signal caused by different R_{ext} settings was eliminated by the utilization of IR [9, 26]. Therefore, the discrepancy of optimal R_{ext} might arise from the different resistance of anodic biofilms to various pollutants. Considering obvious differences in the species and distribution of electricigens under different R_{ext} values [17, 18], the effect of R_{ext} on the sensor sensitivity might be attributed to the discrepancy in anodic microbial communities.

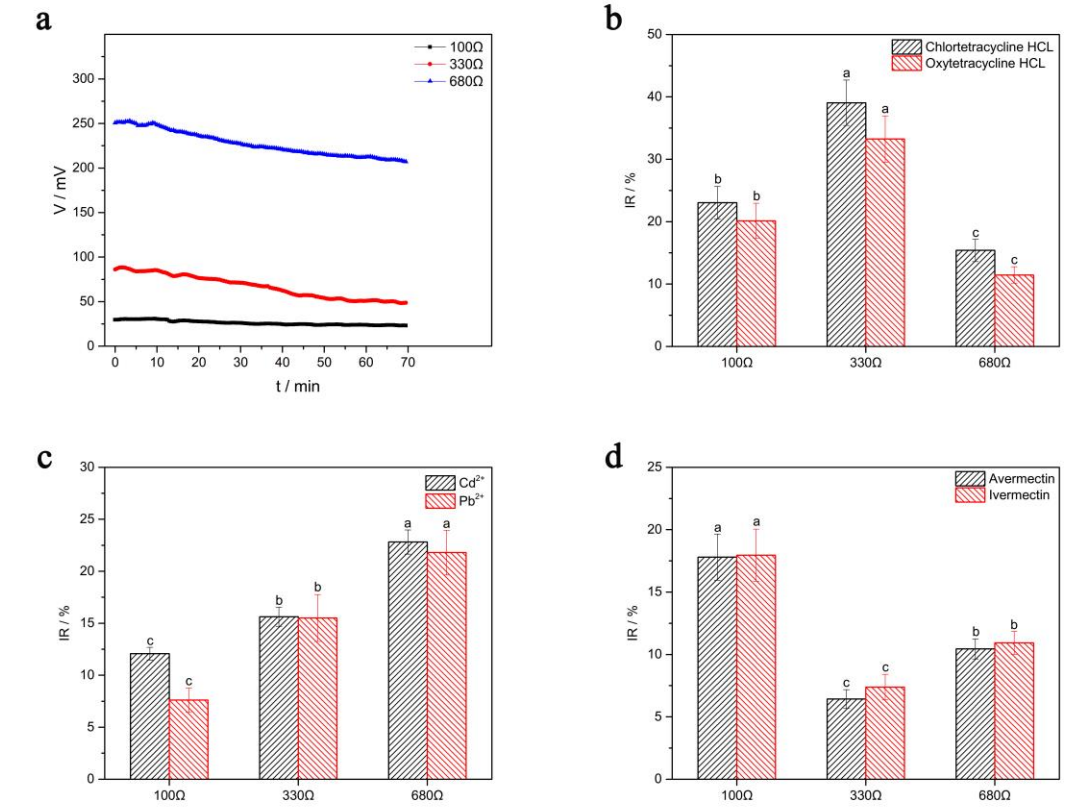

Figure 2. Effect of R_{ext} on the sensor sensitivities to detect various types of pollutants: (a) voltage variations to CTC shock; IR values of the MFC-biosensors exposed to (b) tetracyclines, (c) heavy metals and (d) avermectins. Different alphabets above the columns indicate significant differences ($p<0.05$).

In real aquatic environment, water pollution emergencies usually occur as combined contamination. Coexistence of various types of pollutants would lead to interactions such as synergistic or antagonistic effect [22, 28]. To investigate the change of optimal R_{ext} induced by combined contaminations, MFC1-9 were challenged with two types of combined contaminations including binary metal mixture and inorganic-organic composite pollution. The IR values of MFC-biosensors to the shock of the binary metal mixture (Cd^{2+}+ Pb^{2+}) were presented in Figure 3a. It could be seen that the responses of MFC-biosensors loaded with different R_{ext} settings followed a similar pattern with the results of Cd^{2+} or Pb^{2+} test. The highest sensitivity was still obtained at 680 Ω with an IR of 50.4±3.6%. However, interactions between Cd^{2+} and Pb^{2+} were diverse under different R_{ext} values. To be specific, a remarkable antagonistic effect between Cd^{2+} and Pb^{2+} was recognized in the MFC-biosensors loaded with 100 Ω while a synergistic effect or additive action was present at the other R_{ext} settings. Joint toxicities between Cd^{2+} and Pb^{2+} were also reported by previous studies using various test organisms. When using biotic ligand model to evaluate the bioaccumulation of Cd^{2+} and Pb^{2+} in *Chlamydomonas reinhardtii*, a significant antagonism was found because of a shared bio-uptake pathway [29]. Conversely, combined exposure of Cd^{2+} and Pb^{2+} had an additive effect on hippocampal HT-22 cell [30] while synergistic effect on isopod *Asellus aquaticus* [31]. These observations suggested that the interaction between toxic

components varied for test organisms. Therefore, various interaction between Cd^{2+} and Pb^{2+} in joint toxicity test might also result from the different anodic microbial communities established under different R_{ext} values.

Figure 3b illustrated the IR values to the combined shock of Pb^{2+} and OTC. Synergistic joint toxicity could be observed in all the MFC-biosensors, which was consistent with a previous study [32]. Besides, the strongest response to the mixture of Pb^{2+} and OTC was observed in the MFC-biosensors loaded with 330 Ω, whose value was equal to the optimal R_{ext} for OTC. The results of single pollutant tests have demonstrated that OTC had higher biotoxicity than Pb^{2+} in most cases. Hence, it could be assumed that the optimal R_{ext} for combined contamination might be identical to that of the more toxic component in the mixture.

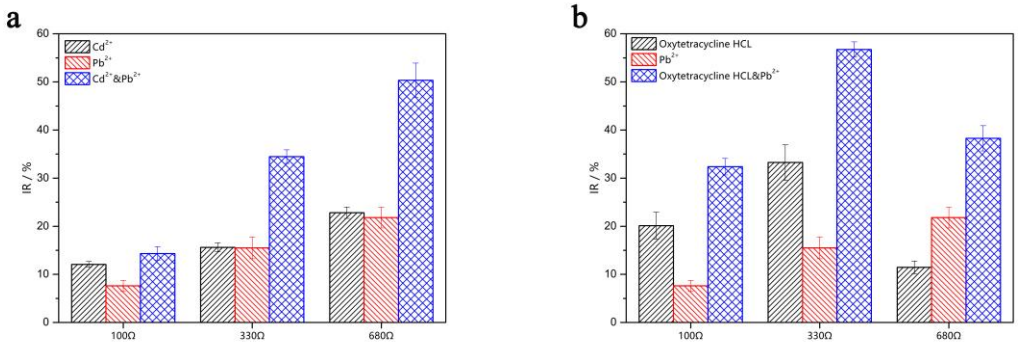

Figure 3. IR values of the MFC-biosensors exposed to combined contaminations: (a) Pb^{2+}+Cd^{2+} and (b) Pb^{2+}+OTC.

3.3 Microbiological mechanism of the effect of external resistance on sensor sensitivity

Toxic pollutants tests suggested that the optimal R_{ext} values for various types of pollutants were different and this discrepancy might be due to the differences in anodic microbial communities under different R_{ext} values. Therefore, comparison of the anodic microbial communities formed under optimal R_{ext} and the corresponding changes after toxic shocks could interpret this discrepancy. In this section, biofilm samples were collected from anode before and after the toxic shock. Detailed information of all the samples was presented in Table 1. High-throughput sequencing technology was employed to analyze the community compositions of all the samples.

Table 1. Treatments and predominant microbial genera of all the samples.

Group	Sample	R_{ext}	Treatment	Predominant microbial genera				
				Geobacter	*Azospirillum*	*Acinetobacter*	*Pseudomonas*	*Oscillibacter*
100N	100N0	MFC10: 100 Ω	Initial	74.65%	2.87%	2.03%	2.70%	2.55%
	100N1	MFC11: 100 Ω	Initial					
100T	100T0	MFC10: 100 Ω	7-day AVM shock	75.25%	2.66%	1.45%	2.61%	1.75%
	100T1	MFC11: 100 Ω	7-day IVM shock	(0.60%↑)	(0.21%↓)	(0.58%↓)	(0.09%↓)	(0.80%↓)
330N	330N0	MFC12: 330 Ω	Initial	70.17%	3.12%	0.72%	10.73%	1.84%
	330N1	MFC13: 330 Ω	Initial					
330T	330T0	MFC12: 330 Ω	7-day CTC shock	68.79%	2.27%	1.91%	9.44%	0.92%
	330T1	MFC13: 330 Ω	7-day OTC shock	(1.38%↓)	(0.85%↓)	(1.19%↑)	(1.29%↓)	(0.92%↓)
680N	680N0	MFC14: 680 Ω	Initial	54.05%	12.22%	6.98%	3.65%	0.55%
	680N1	MFC15: 680 Ω	Initial					
680T	680T0	MFC14: 680 Ω	7-day Cd^{2+} shock	58.12%	9.68%	3.00%	4.01%	0.64%
	680T1	MFC15: 680 Ω	7-day Pb^{2+} shock	(4.07%↑)	(2.54%↓)	(3.98%↓)	(0.36%↑)	(0.09%↑)

Rarefaction curves of all the samples were presented in Figure 4a. For each sample, the number of OTUs seemed to reach a plateau when more than 50,000 clones were sequenced, which indicated that the sequence data could cover the majority of the anodic microbial populations. Then PCoA was applied to all the samples at a classification level of OTU (Figure 4b). PC1 and PC2 accounted for over 77% of the variations in the anodic community structures of MFC10-15. Hence the differences in community structures among the samples could be truly reflected. As shown in Figure 4b, samples of MFCs operated at different R_{ext} settings were widely separated, which suggested that distinct anodic communities were formed under different R_{ext} values. This observation was consistent with the previous studies [15, 17, 18]. Moreover, all types of toxic shocks led to remarkable shifts in community structures (Figure 4b), which resulted from the exposures to toxic pollutants. So far, the influences of heavy metal contamination and tetracycline residue on the community compositions of soil microbes or aquatic microorganisms have been the subject of extensive studies in the area of environment pollution [33, 34], but the impact of avermectins was seldom

concerned. In this study, a remarkable alternation in anodic microbial communities to the shocks of avermectins was noticed. This phenomenon suggested that with the widespread use of avermectins in agriculture, the impact of residual avermectins in soil and water on their microbial community deserved more attention.

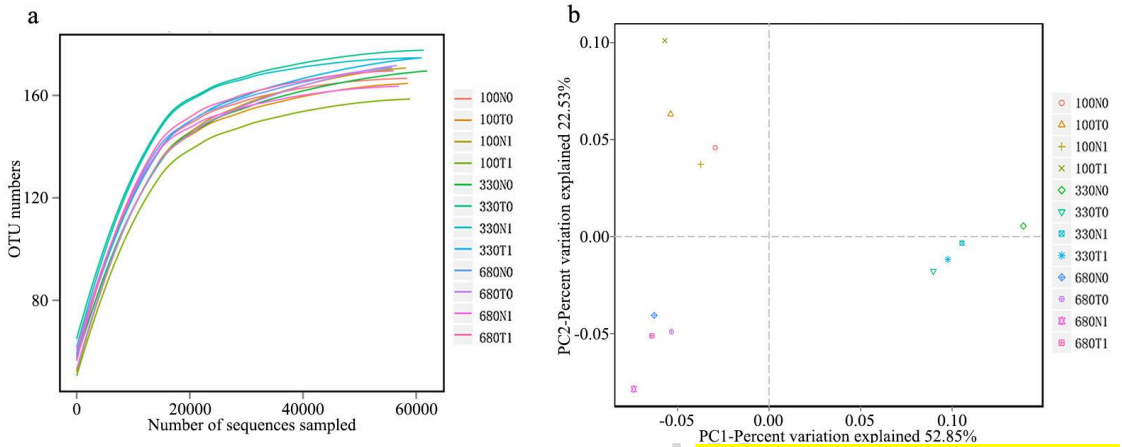

Figure 4. (a) Rarefaction curves and (b) PCoA plot of all the samples. Detailed information of all the samples was presented in Table 1.

Community compositions of all the samples on the classification level of genus were presented in Figure 5. 100N, 330N and 680N represented the biofilm samples collected from the MFCs stably operated at 100 Ω, 330 Ω and 680 Ω. The majorities of genera in these samples were *Geobacter* (54.05-74.65%), *Azospirillum* (2.87-12.22%), *Pseudomonas* (2.70-10.73%), *Acinetobacter* (0.72-6.98%) and *Oscillibacter* (0.55-2.55%), and these genera showed diverse preferences for R_{ext}. The relative abundance of *Geobacter* achieved 74.65% in 100N, then followed by 70.17% in 330N and 54.05% in 680N. This was because that a relatively high anodic potential was more suitable for the growth of *Geobacter* [35]. The proportions of *Oscillibacter* in MFCs loaded with different R_{ext} values followed a similar trend. Despite relatively low abundance, a decrease from 2.55% (100N) to only 0.55% (680N) could be observed. On the contrary, both *Azospirillum* and *Acinetobacter* occupied high proportions in 680N than the other samples. This suggested a better survival of these two genera under a low anodic potential. Besides, unlike the genera discussed above, *Pseudomonas* accounted for 10.73% of the microbial population in 330N while in 100N and 680N it only made up 2.70% and 3.65% of the total communities. A previous study reported that *Pseudomonas* showed distinct electrochemical activities at different potentials [36]. Results in this study further manifested that the enrichment of *Pseudomonas* was only available in a limited scale of R_{ext} settings.

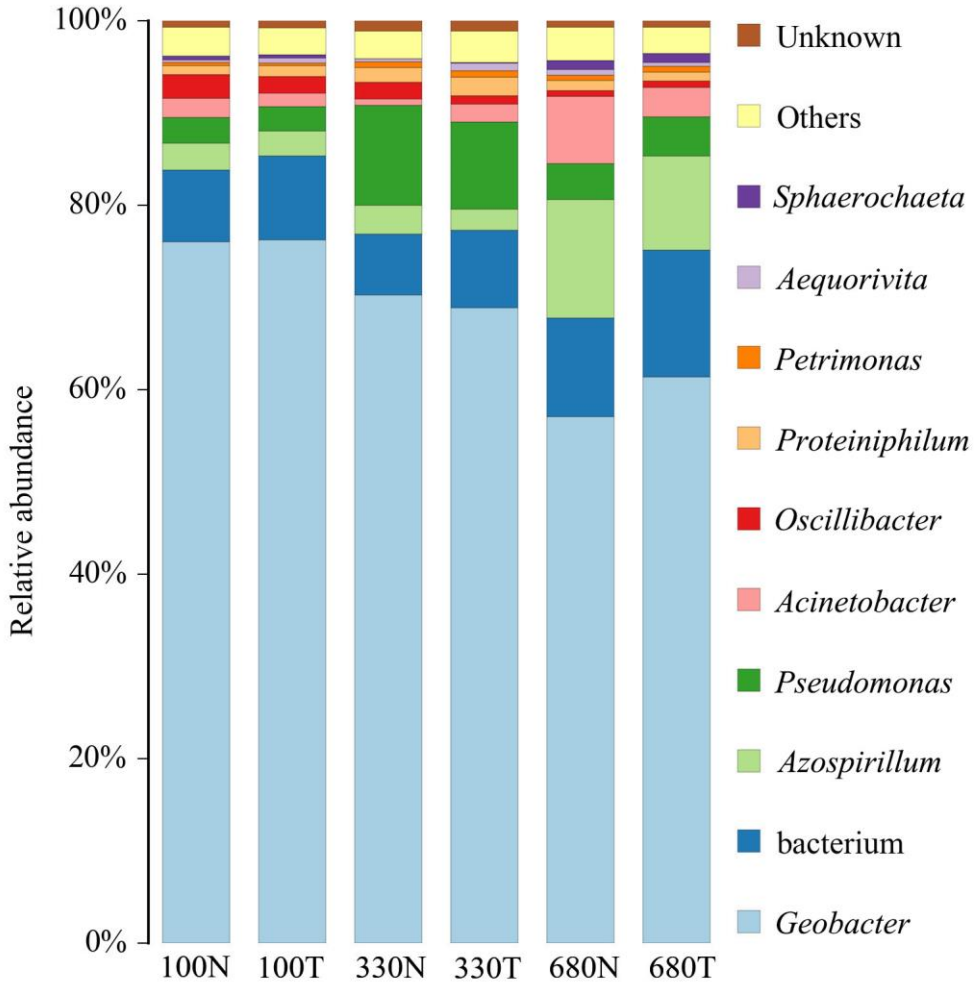

Figure 5. Community compositions of all the samples on the classification level of genus. Detailed information of all the samples was presented in Table 1.

680T represented the biofilm samples collected from the MFCs loaded with 680Ω after heavy metal exposures for seven days. Sharp decreases induced by heavy metals in the relative abundances of *Azospirillum* and *Acinetobacter* could be clearly recognized in 680T (Figure 5). The total proportion of these two genera reduced from 19.20% (680N) to 12.68% (680T), which indicated the susceptibilities to heavy metal pollutants. *Azospirillum* was commonly identified as a genus of nitrogen-fixing bacteria. Five strains of *Azospirillum* isolated from rice root samples were all sensitive to Cd^{2+} and Pb^{2+} [37]. This phenomenon was also observed by Bashan et al. [38]. Similarly, *Acinetobacter* was intolerant to heavy metals as well. Serious heavy metal contamination significantly reduced the abundance of *Acinetobacter* in soil [39]. Since both *Azospirillum* and *Acinetobacter* were electrochemically active [40, 41], the susceptibilities to heavy metals of these two genera might account for the highest sensitivity to Cd^{2+} and Pb^{2+} in MFC-biosensors loaded with 680 Ω. On the other side, *Azospirillum* and *Acinetobacter* were reported to be resistant to many antibiotics [38, 42]. Therefore, the enrichments of these two genera in 680N might deteriorate the sensor sensitivity to detect antibiotics pollutants.

Geobacter and *Pseudomonas* were the predominant genera in 330N, which totally accounted for 80.9% of the microbial populations. After 7-day tetracyclines shocks, the proportions of *Geobacter* and *Pseudomonas* decreased to 68.79% and 9.44% respectively, which were around 98.03% and 87.98% of the initial abundances. This phenomenon indicated an obvious sensitivity of *Pseudomonas* to tetracyclines, which was in accord with the observations in previous studies. Increasing tetracycline concentration in soil significantly decreased the proportion of *Pseudomonas* [43]. Moreover, the minimum inhibitory concentration of tetracycline to a wild-type *Pseudomonas aeruginosa* isolated from brown algae was only 3.34 μg/mL, which suggested an obvious susceptibility [44]. *Pseudomonas* was proved to be an electroactive microorganism by an early study [45]. Therefore, the significant voltage drops induced by tetracyclines shocks in the MFC-biosensors loaded with 330 Ω might be primarily attributed to the susceptibility of *Pseudomonas*. However, both *Geobacter* and *Pseudomonas* were metal tolerant genera. *Geobacter* was one of the dissimilatory metal reduction microorganisms, which was capable of reducing ferric iron and tetravalent manganese [46]. As for *Pseudomonas*, it could survive an exposure of 20 mg/kg Cd^{2+} pollution in soil [47]. These observations suggested that the relatively poor responses to heavy metals pollutants in the MFC-biosensors loaded with 330 Ω might be due to the predominant existence of these two genera.

The biofilm samples collected from the MFCs loaded with 100 Ω before and after toxic exposures were denoted by 100N and 100T. Compared with 100N, the relative abundance of *Oscillibacter* reduced to 1.75% after 7-day avermectins shocks, which was only 68.63% of the initial proportion. This phenomenon suggested the susceptibility to avermectins in *Oscillibacter*. *Oscillibacter* was also reported to be probably contributive to the electricity generation by a recent study [48]. Hence, the variation in the proportion of *Oscillibacter* might partly explain the apparent voltage decay in 100 Ω MFC-biosensors after avermectins shock. Though few literatures on the biotoxicity of avermectins to *Oscillibacter* were published, the susceptibility to multiple antibiotics such as vancomycin and cefoperazone has been revealed [49, 50]. Besides, a very recent study reported that *Oscillibacter* significantly proliferated in the intestinal microorganisms collected from the mice receiving Pb^{2+} polluted water, which indicated a better survival of this genus under heavy metal exposure [51]. Given that the metal tolerant genera *Geobacter* and *Pseudomonas* occupied 77.35% of the microbial population in 100N, the lowest sensitivity to heavy metals in the MFC-biosensors loaded with 100 Ω might be due to the great abundance of *Geobacter*, *Pseudomonas* and *Oscillibacter*.

Toxic pollutants tests and microbial community analysis revealed that R_{ext} could obviously affect anodic microbial community and further impact sensor sensitivity. Hence, adjusting of R_{ext} to enrich certain electricigens which were sensitive to target toxic agents could enhance the sensitivity to detect a specific type of pollutants. For instance, at the outlet carrying electroplating wastewater, the enrichment of *Azospirillum* or *Acinetobacter* was favorable for alert of heavy metal contamination. As for breeding industry where antibiotics were extensively used, the proliferation of

Pseudomonas and *Oscillibacter* could be employed to improve the response to detect potential antibiotic pollution. Furthermore, this study exploited the possibility to distinguish pollutant type by MFC-biosensors. A sensor array composed of a multitude of MFCs with different microbial communities could be constructed for water quality monitoring of complicated contaminated wastewater. Comparative analysis of the responses to toxic shock in the sensor array might be able to discriminate pollutant type. Further studies should be focused on enlarging the detection range and constructing the sensor array to develop a practical strategy for identification of pollutant type in combined contamination.

4. Conclusions

This study demonstrated that the effect of R_{ext} on sensor sensitivity varied for pollutant type. For single pollutants, the highest sensitivities for detection of avermectins, tetracyclines and heavy metals pollutants were obtained in 100 Ω, 330 Ω and 680 Ω MFC-biosensors, respectively. While for the combined contaminations, the optimal R_{ext} might be identical to that of the more toxic component in the mixture. The discrepancy in optimal R_{ext} was attributed to the differences in anodic microbial communities. Different proportions of *Geobacter*, *Azospirillum*, *Pseudomonas*, *Acinetobacter* and *Oscillibacter* at various R_{ext} settings led to the discrepancies in sensor sensitivities. Future studies will be concerned about the further optimization of anode microbial community to enhance the sensitivity to specific toxic agents and the construction of a sensor-array to distinguish pollutant type.

Acknowledgements

This work was financially supported by grants from the National Natural Science Foundation of China [31770135]; Beijing Municipal Science & Technology Commission [Z171100000717013]; National Undergraduate's Innovation and Entrepreneurship Training Program [201610006085]; and the Fundamental Research Funds for the Central Universities.

Associated Content

SUPPLEMENTARY MATERIAL

The schematic diagram and prototype of the MFC-biosensor in this research were shown in Fig. A1. Output voltages of the MFC-biosensors with various R_{ext} settings when operated with non-toxic anolyte were shown in Fig. A2.

References

[1]. S.H.A. Hassan, S.W. Van Ginkel, M.A.M. Hussein, R. Abskharon, S.-E. Oh, Toxicity assessment using different bioassays and microbial biosensors, Environ. Int. 92-93 (2016) 106-118.

[2]. Y. Jiang, X.F. Yang, P. Liang, P.P. Liu, X. Huang, Microbial fuel cell sensors for water quality early warning systems: Fundamentals, signal resolution, optimization and future challenges, Renew. Sust. Energ. Rev. 81 (2018) 292-305.

[3]. H.J. Yang, M.H. Zhou, M.M. Liu, W.L. Yang, T.Y. Gu, Microbial fuel cells for biosensor applications, Biotechnol. Lett. 37 (2015) 2357-2364.

[4]. B.E. Logan, Exoelectrogenic bacteria that power microbial fuel cells, Nat. Rev. Microbiol. 7 (2009) 375-381.

[5]. M. Kim, M.S. Hyun, G.M. Gadd, H.J. Kim, A novel biomonitoring system using microbial fuel cells, J. Environ. Monit. 9 (2007) 1323-1328.

[6]. N.E. Stein, H.V.M. Hamelers, C.N.J. Buisman, The effect of different control mechanisms on the sensitivity and recovery time of a microbial fuel cell based biosensor, Sensor. Actuat. B-Chem. 171 (2012) 816-821.

[7]. M. Di Lorenzo, A.R. Thomson, K. Schneider, P.J. Cameron, I. Ieropoulos, A small-scale air-cathode microbial fuel cell for on-line monitoring of water quality, Biosens. Bioelectron. 62 (2014) 182-188.

[8]. Z.H. Xu, B.C. Liu, Q.C. Dong, Y. Lei, Y. Li, J. Ren, J. McCutcheon, B.K. Li, Flat microliter membrane-based microbial fuel cell as "on-line sticker sensor" for self-supported *in situ* monitoring of wastewater shocks, Bioresour. Technol. 197 (2015) 244-251.

[9]. X. Wang, N.S.J. Gao, Q.X. Zhou, Concentration responses of toxicity sensor with *Shewanella oneidensis* MR-1 growing in bioelectrochemical systems, Biosens. Bioelectron. 43 (2013) 264-267.

[10]. Y.J. Shen, M. Wang, I.S. Chang, H.Y. Ng, Effect of shear rate on the response of microbial fuel cell toxicity sensor to Cu(II), Bioresour. Technol. 136 (2013) 707-710.

[11]. Y. Jiang, P. Liang, C.Y. Zhang, Y.H. Bian, X.F. Yang, X. Huang, P.R. Girguis, Enhancing the response of microbial fuel cell based toxicity sensors to Cu(II) with the applying of flow-through electrodes and controlled anode potentials, Bioresour. Technol. 190 (2015) 367-372.

[12]. O. Modin, B.M. Wilén, A novel bioelectrochemical BOD sensor operating with voltage input, Water Res. 46 (2012) 6113-6120.

[13]. Y. Yi, B.Z. Xie, T. Zhao, H. Liu, Comparative analysis of microbial fuel cell based biosensors developed with a mixed culture and *Shewanella loihica* PV-4 and underlying biological mechanism, Bioresour. Technol. 265 (2018) 415-421.

[14]. Y. Yi, X.Y. Li, X.H. Jiang, B.Z. Xie, H. Liu, D.W. Liang, Y. Zhu, Optimization study of a microbial fuel cell (MFC)-based biosensor, The 2015 International Conference on Materials Engineering and Environmental Science, 2015, pp. 643-652.

[15]. K.P. Katuri, K. Scott, I.M. Head, C. Picioreanu, T.P. Curtis, Microbial fuel cells meet with external resistance, Bioresour. Technol. 102 (2011) 2758-2766.

[16]. M. Li, M.H. Zhou, X.Y. Tian, C.L. Tan, C.T. McDaniel, D.J. Hassett, T.Y. Gu, Microbial fuel cell (MFC) power performance improvement through enhanced microbial electrogenicity, Biotechnol. Adv. 36 (2018) 1316-1327.

[17]. H. Kim, B. Kim, J. Kim, T. Lee, J. Yu, Electricity generation and microbial community in microbial fuel cell using low-pH distillery wastewater at different external resistances, J. Biotechnol. 186 (2014) 175-180.

[18]. D.Y. Lyon, F. Buret, T.M. Vogel, J.-M. Monier, Is resistance futile? Changing external resistance does not improve microbial fuel cell performance, Bioelectrochemistry 78 (2010) 2-7.

[19]. W.E. Balch, G.E. Fox, L.J. Magrum, C.R. Woese, R.S. Wolfe, *Methanogens*: reevaluation of a unique biological group, Microbiol. Rev. 43 (1979) 260-296.

[20]. Y. Jiang, P. Liang, P.P. Liu, Y.H. Bian, B. Miao, X.L. Sun, H.L. Zhang, X. Huang, Enhancing signal output and avoiding BOD/toxicity combined shock interference by operating a microbial fuel cell sensor with an optimized background concentration of organic matter, Int. J. Mol. Sci. 17 (2016) 1392-1399.

[21]. S.A. Cheng, B.E. Logan, Ammonia treatment of carbon cloth anodes to enhance power generation of microbial fuel cells, Electrochem. Commun. 9 (2007) 492-496.

[22]. G.Y. Gao, J. Qian, D.Y. Fang, Y. Yu, J.F. Zhi, Development of a mediated whole cell-based electrochemical biosensor for joint toxicity assessment of multi-pollutants using a mixed microbial consortium, Anal. Chim. Acta 924 (2016) 21-28.

[23]. B.Z. Xie, B.J. Liu, Y. Yi, L.G. Yang, D.W. Liang, Y. Zhu, H. Liu, Microbiological mechanism of the improved nitrogen and phosphorus removal by embedding microbial fuel cell in Anaerobic-Anoxic-Oxic wastewater treatment process, Bioresour. Technol. 207 (2016) 109-117.

[24]. Y. Yin, G.T. Huang, Y.R. Tong, Y.D. Liu, L.H. Zhang, Electricity production and electrochemical impedance modeling of microbial fuel cells under static magnetic field, J. Power Sources 237 (2013) 58-63.

[25]. X.P. Zhu, J.C. Tokash, Y.Y. Hong, B.E. Logan, Controlling the occurrence of power overshoot by adapting microbial fuel cells to high anode potentials, Bioelectrochemistry 90 (2013) 30-35.

[26]. T. Li, X. Wang, L. Zhou, J. An, J. Li, N. Li, H. Sun, Q. Zhou, Bioelectrochemical sensor using living biofilm to in situ evaluate flocculant toxicity, ACS Sens. 1 (2016) 1374-1379.

[27]. L. Zhang, X. Zhu, J. Li, Q. Liao, D.D. Ye, Biofilm formation and electricity generation of a microbial fuel cell started up under different external resistances, J. Power Sources 196 (2011) 6029-6035.

[28]. Y. Yi, X.Y. Li, X.H. Jiang, B.Z. Xie, H. Liu, D.W. Liang, Y. Zhu, Assessing the solitary and joint biotoxicities of heavy metals and acephate using microbial fuel

cell, The 2015 International Conference on Advances in Energy, Environment and Chemical Engineering, 2015, pp. 694-699.

[29]. Y. Zhou, L. Zhu, J.F. Feng, G. Yang, Validation of the biotic ligand model (BLM) to Pb and Cd, and their mixtures, Asian J. Ecotoxicol. 10 (2015) 47-54.

[30]. V. Karri, V. Kumar, D. Ramos, E. Oliveira, M. Schuhmacher, An in vitro cytotoxic approach to assess the toxicity of heavy metals and their binary mixtures on hippocampal HT-22 cell line, Toxicol. Lett. 282 (2018) 25-36.

[31]. M. Van Ginneken, M. De Jonge, L. Bervoets, R. Blust, Uptake and toxicity of Cd, Cu and Pb mixtures in the isopod *Asellus aquaticus* from waterborne exposure, Sci. Total Environ. 537 (2015) 170-179.

[32]. M.L. Gao, Q. Zhou, W.H. Song, X.J. Ma, Combined effects of oxytetracycline and Pb on earthworm *Eisenia fetida*, Environ. Toxicol. Pharmacol. 37 (2014) 689-696.

[33]. C.J. Feng, A.Y. Hu, S.H. Chen, C.P. Yu, A decentralized wastewater treatment system using microbial fuel cell techniques and its response to a copper shock load, Bioresour. Technol. 143 (2013) 76-82.

[34]. Y.H. Xiong, M. Harb, P.Y. Hong, Performance and microbial community variations of anaerobic digesters under increasing tetracycline concentrations, Appl. Microbiol. Biotechnol. 101 (2017) 5505-5517.

[35]. H. Richter, K.P. Nevin, H.F. Jia, D.A. Lowy, D.R. Lovley, L.M. Tender, Cyclic voltammetry of biofilms of wild type and mutant *Geobacter sulfurreducens* on fuel cell anodes indicates possible roles of OmcB, OmcZ, type IV pili, and protons in extracellular electron transfer, Energy Environ. Sci. 2 (2009) 506-516.

[36]. S. Hintermayer, S.Q. Yu, J.O. Krömer, D. Weuster-Botz, Anodic respiration of *Pseudomonas putida* KT2440 in a stirred-tank bioreactor, Biochem. Eng. J. 115 (2016) 1-13.

[37]. M.A. Akond, Z.U.M. Khan, Role of carbon sources and heavy metals on growth and nitrogen fixing potential of *Azospirillum* and the effect of *Azospirillum* strains on vegetative growth of rice, J. Environ. Sci. 3 (2005) 1-8.

[38]. Y. Bashan, G. Holguin, L.E. de-Bashan, *Azospirillum*-plant relationships: physiological, molecular, agricultural, and environmental advances (1997-2003), Can. J. Microbiol. 50 (2004) 521-577.

[39]. H.H. Guo, M. Nasir, J.L. Lv, Y.C. Dai, J.K. Gao, Understanding the variation of microbial community in heavy metals contaminated soil using high throughput sequencing, Ecotoxicol. Environ. Saf. 144 (2017) 300-306.

[40]. Y. Xiao, Y. Zheng, S. Wu, E.H. Zhang, Z. Chen, P. Liang, X. Huang, Z.H. Yang, I.S. Ng, B.Y. Chen, F. Zhao, Pyrosequencing reveals a core community of anodic bacterial biofilms in bioelectrochemical systems from China, Front. Microbiol. 6 (2015) 1-12.

[41]. E.R. Zhang, Q.L. Yu, W.J. Zhai, F. Wang, K. Scott, High tolerance of and removal of cefazolin sodium in single-chamber microbial fuel cells operation, Bioresour. Technol. 249 (2018) 76-81.

[42]. J. Hrenovic, G. Durn, M.S. Music, S. Dekic, T. Troskot-Corbic, D. Skoric, Extensively and multi drug-resistant *Acinetobacter baumannii* recovered from technosol at a dump site in Croatia, Sci. Total Environ. 607 (2017) 1049-1055.

[43]. M.L. Duan, H.C. Li, J. Gu, X.X. Tuo, W. Sun, X. Qian, X.J. Wang, Effects of biochar on reducing the abundance of oxytetracycline, antibiotic resistance genes, and human pathogenic bacteria in soil and lettuce, Environ. Pollut. 224 (2017) 787-795.

[44]. X.J. He, H.-M. Hwang, W.G. Aker, P. Wang, Y.F. Lin, X.L. Jiang, X.Y. He, Synergistic combination of marine oligosaccharides and azithromycin against *Pseudomonas aeruginosa*, Microbiol. Res. 169 (2014) 759-767.

[45]. T.H. Pham, N. Boon, K. De Maeyer, M. Höefte, K. Rabaey, W. Verstraete, Use of *Pseudomonas* species producing phenazine-based metabolites in the anodes of microbial fuel cells to improve electricity generation, Appl. Microbiol. Biotechnol. 80 (2008) 985-993.

[46]. B. Yan, B.A. Methé, D.R. Lovley, J. Krushkal, Computational prediction of conserved operons and phylogenetic footprinting of transcription regulatory elements in the metal-reducing bacterial family *Geobacteraceae*, J. Theor. Biol. 230 (2004) 133-144.

[47]. L. Chen, S.L. Luo, X.J. Li, Y. Wan, J.L. Chen, C.B. Liu, Interaction of Cd-hyperaccumulator *Solanum nigrum* L. and functional endophyte *Pseudomonas* sp. Lk9 on soil heavy metals uptake, Soil Biol. Biochem. 68 (2014) 300-308.

[48]. Y.B. Jiang, W.H. Zhong, C. Han, H. Deng, Characterization of electricity generated by soil in microbial fuel cells and the isolation of soil source exoelectrogenic bacteria, Front. Microbiol. 7 (2016) 1-10.

[49]. S.F. Clarke, E.F. Murphy, O. O'Sullivan, R.P. Ross, P.W. O'Toole, F. Shanahan, P.D. Cotter, Targeting the microbiota to address diet-induced obesity: a time dependent challenge, PLoS One 8 (2013) 1-9.

[50]. J.R.E. Downward, N.R. Falkowski, K.L. Mason, R. Muraglia, G.B. Huffnagle, Modulation of post-antibiotic bacterial community reassembly and host response by *Candida albicans*, Sci. Rep. 3 (2013) 1-11.

[51]. Q.X. Zhai, T.Q. Li, L.L. Yu, Y. Xiao, S.S. Feng, J.P. Wu, J.X. Zhao, H. Zhang, W. Chen, Effects of subchronic oral toxic metal exposure on the intestinal microbiota of mice, Sci. Bull. 62 (2017) 831-840.

Table 1. Treatments and predominant microbial genera of all the samples.

Group	Sample	R_{ext}	Treatment	Predominant microbial genera				
				Geobacter	*Azospirillum*	*Acinetobacter*	*Pseudomonas*	*Oscillibacter*
100N	100N0	MFC10: 100 Ω	Initial	74.65%	2.87%	2.03%	2.70%	2.55%
	100N1	MFC11: 100 Ω	Initial					
100T	100T0	MFC10: 100 Ω	7-day AVM shock	75.25%	2.66%	1.45%	2.61%	1.75%
	100T1	MFC11: 100 Ω	7-day IVM shock	（0.60%↑）	（0.21%↓）	（0.58%↓）	（0.09%↓）	（0.80%↓）
330N	330N0	MFC12: 330 Ω	Initial	70.17%	3.12%	0.72%	10.73%	1.84%
	330N1	MFC13: 330 Ω	Initial					
330T	330T0	MFC12: 330 Ω	7-day CTC shock	68.79%	2.27%	1.91%	9.44%	0.92%
	330T1	MFC13: 330 Ω	7-day OTC shock	（1.38%↓）	（0.85%↓）	（1.19%↑）	（1.29%↓）	（0.92%↓）
680N	680N0	MFC14: 680 Ω	Initial	54.05%	12.22%	6.98%	3.65%	0.55%
	680N1	MFC15: 680 Ω	Initial					
680T	680T0	MFC14: 680 Ω	7-day Cd^{2+} shock	58.12%	9.68%	3.00%	4.01%	0.64%
	680T1	MFC15: 680 Ω	7-day Pb^{2+} shock	（4.07%↑）	（2.54%↓）	（3.98%↓）	（0.36%↑）	（0.09%↑）

Highlights

- Optimal external resistance of MFC-biosensor varies with the type of pollutants.
- The optimal external resistance for detecting heavy metals is 680 Ω.
- The optimal value for avermectins is 100 Ω while 330 Ω for tetracyclines.
- The discrepancy is attributed to the differences in anodic microbial communities.